

Retention time and dispersion associated with submerged aquatic canopies

H. Nepf,¹ M. Ghisalberti,² B. White,³ and E. Murphy¹

Received 20 July 2006; revised 28 November 2006; accepted 1 December 2006; published 18 April 2007.

[1] The shear layer at the top of a submerged canopy generates coherent vortices that control exchange between the canopy and the overflowing water. Unlike free shear layers, the vortices in a canopy shear layer do not grow continuously downstream but reach and maintain a finite scale determined by a balance between shear production and canopy dissipation. This balance defines the length scale of vortex penetration into the canopy, δ_e , and the region of rapid exchange between the canopy and overflow. Deeper within the canopy, transport is constrained by smaller turbulence scales. A two-box canopy model is proposed on the basis of the length scale δ_e . Using diffusivity and exchange rates defined in previous studies, the model predicts the timescale required to flush the canopy through vertical exchange over a range of canopy density and height. The predicted canopy retention times, which range from minutes to an hour, are consistent with canopy retention inferred from tracer observations in the field and comparable to retention times for some hyporheic regions. The timescale for vertical exchange, along with the in-canopy velocity, determines the minimum canopy length for which vertical exchange dominates water renewal. Shorter canopies renew interior water through longitudinal advection. Finally, canopy water retention influences longitudinal dispersion through a transient storage process. When vertical exchange controls canopy retention, the transient storage dispersion increases with canopy height. When longitudinal advection controls water renewal, dispersion increases with canopy patch length.

Citation: Nepf, H., M. Ghisalberti, B. White, and E. Murphy (2007), Retention time and dispersion associated with submerged aquatic canopies, *Water Resour. Res.*, 43, W04422, doi:10.1029/2006WR005362.

1. Introduction

[2] The primary impact of submerged vegetation is an increase in flow resistance and subsequent reduction in conveyance capacity [e.g., *Kouwen and Unny*, 1973; *Kouwen*, 1990; *Wu et al.*, 1999], so that for many years vegetation has been removed from river channels to accelerate the passage of peak flows. However, aquatic macrophytes can have a positive influence on water quality by removing nutrients and producing oxygen in stagnant regions [e.g., *Chambers and Prepas*, 1994; *Mars et al.*, 1999; *Wilcock et al.*, 1999; *Schultz et al.*, 2002]. Submerged canopies also create regions of diminished flow that promote sedimentation and the retention of particulate nutrients [e.g., *Triska et al.*, 1989; *Sand-Jensen*, 1998; *Tsujimoto*, 2000]. More broadly, submerged vegetation may contribute to hydrologic storage [*Harvey et al.*, 2003]. Hydrologic storage occurs in regions of diminished flow in which water can remain in contact with biologically and geochemically active surfaces for an extended time before

moving downstream. The hyporheic zone, abundant with reacting grain surfaces, is probably the most important region of storage. However, macrophytes, which take up nutrients and support nutrient-hungry colonies of periphyton, also have great potential for nutrient removal [*Harvey et al.*, 2005].

[3] The timescale over which water is retained in storage is called the hydrologic retention. Longer periods of retention allow for more extensive chemical reaction and thus greater nutrient removal. Although aquatic canopies are recognized as a component of hydrologic storage [*Harvey et al.*, 2003], there is no model with which to predict hydrologic retention associated with canopies. This paper will build on existing knowledge of canopy hydrodynamics to construct a physical model for water renewal within a submerged canopy. Section 2 develops a scaling law for canopy shear layers, which is applied in section 3 to construct a two-box model for canopy flushing. Section 4 presents the canopy retention predicted for a range of canopy morphology and channel slope representative of field conditions. The predicted timescales are comparable to available field estimates for aquatic canopy retention. Finally, section 5 discusses the implications of canopy retention for longitudinal dispersion.

2. Physical Basis for a Canopy Flushing Model

[4] The dominant feature of flow near the edge of a submerged canopy is a region of strong shear, created by the discontinuity in drag. The velocity profile in this region

¹Department of Civil and Environmental Engineering, Massachusetts Institute of Technology, Cambridge, Massachusetts, USA.

²School of Environmental Systems Engineering, University of Western Australia, Crawley, Western Australia, Australia.

³Woods Hole Oceanographic Institution, Woods Hole, Massachusetts, USA.

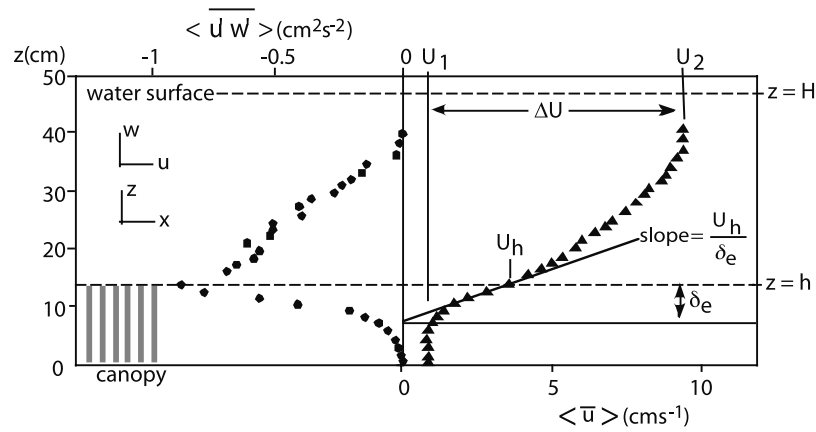


Figure 1. Velocity (triangles) and Reynolds' stress (circles) in and above a submerged canopy (run I [Ghisalberti and Nepf, 2004]). A drag discontinuity at the canopy top ($z = h$) creates a shear layer with velocity difference $\Delta U = U_2 - U_1$. The shear-scale turbulence penetrates into the canopy a distance δ_e from the canopy top.

resembles a free shear layer, including an inflection point near the top of the canopy (Figure 1). The analogy between canopy shear layers and free shear layers was first shown for terrestrial [Raupach *et al.*, 1996] and later aquatic canopies [Ghisalberti and Nepf, 2002]. Katul *et al.* [2002] extended the analogy to gravel bed streams, using it as a basis for predicting bed resistance.

[5] A free shear layer is characterized by large coherent vortices that form via Kelvin-Helmholtz (K-H) instability. These vortices dominate the transport across the layer [Brown and Roshko, 1974; Winant and Browand, 1974], and the exchange of scalars and momentum between the canopy and overlying flow [Ghisalberti and Nepf, 2004, 2005]. In a free shear layer the vortices grow continually downstream, predominantly through vortex pairing [Winant and Browand, 1974]. In a canopy shear layer, however, the vortices reach a fixed scale and a fixed penetration into the canopy (δ_e in Figure 1) at a short distance from the canopy's leading edge [Ghisalberti and Nepf, 2004]. The penetration length, δ_e , segregates the canopy into an upper layer of rapid renewal and lower layer of slow renewal [Nepf and Vivoni, 2000].

[6] A prediction of δ_e may be derived from conservation laws for turbulent kinetic energy. In particular, we are interested in the turbulent kinetic energy budget at the shear layer scale, which represents the shear-scale vortices. Consider a canopy with stem density n (stems per area) and frontal area per volume $a = nd$, where d is the stem diameter. The canopy height, h , is less than the flow depth, H , so that open flow exists above the canopy, as in Figure 1. The principal flow, u , is along the x coordinate, with v (v) and w (w) denoting lateral and vertical directions, respectively.

[7] Because the flow is forced to move around each stem, the velocity field within the canopy is spatially heterogeneous at the stem scale. A horizontal averaging scheme, described by Raupach and Shaw [1982], is used to account for this heterogeneity. Following their notation, the velocity (u, v, w) and pressure (p) fields are first decomposed into a time average (overbar) and deviations from the time average (single prime). The time-averaged quantities are further decomposed into the spatial mean in a horizontal plane (angle bracket) and deviations from the spatial mean

(double prime). The horizontal average is taken over a length scale greater than the stem spacing. Applying this averaging scheme, the equation for turbulent kinetic energy (k) becomes [e.g., Raupach and Shaw, 1982].

$$\begin{aligned} \frac{D}{Dt} \langle \bar{k} \rangle = & - \langle \overline{u'w'} \rangle \frac{\partial}{\partial z} \langle \bar{u} \rangle - \frac{\partial}{\partial z} \langle \overline{w'k_s} \rangle \\ & - \frac{1}{\rho} \frac{\partial}{\partial z} \langle \overline{w'p'} \rangle - \frac{\partial}{\partial z} \langle \overline{w'k_s''} \rangle - e_c - e_v \end{aligned} \quad (1)$$

[8] To predict the evolution of the shear-scale vortices, we consider the contribution of each term to that scale. The first term on the right-hand side of equation (1) represents shear production, which contributes positively at the shear layer scale (i.e., positive over the entire layer). The second and third terms represent vertical transport within the shear layer associated with turbulence and pressure fluctuations, respectively. Using an LES model, Dwyer *et al.* [1997] showed that these two terms redistribute turbulence within the shear layer but do not provide a net gain or loss at the shear layer scale (e.g., their Figure 2). In fact, these terms reflect the action of the shear-scale vortices on smaller-scale turbulence. The fourth term is a new term arising from spatial correlations in the time-averaged field. Poggi *et al.* [2004b] has shown that this term, called dispersive transport, is negligible for $ah > 0.1$. In the following discussion we restrict our attention to canopies with $ah > 0.1$, and neglect this term. The canopy dissipation, e_c , represents the damping of turbulence by canopy drag [e.g., Wilson, 1988].

$$e_c = \frac{1}{2} C_D a \langle \bar{u} \rangle \left(2 \langle \overline{u'^2} \rangle + \langle \overline{v'^2} \rangle + \langle \overline{w'^2} \rangle \right) \quad (2)$$

Here C_D is a canopy drag coefficient, which may differ in magnitude from the drag coefficient of an isolated stem of the same form [see, e.g., Brunet *et al.*, 1994; Nepf, 1999; Poggi *et al.*, 2004c]. This term drains energy from the shear layer scale. The form-drag fraction of (2) represents a conversion of shear-scale turbulence to stem wake turbulence. The stem wake turbulence contributes to diffusivity in the lower regions of the canopy, as discussed below.

Table 1. Laboratory and Field Data Used to Evaluate the Canopy Shear Layer Parameter (Equation (4))^a

Experimental Study	Flow Conditions	Figure Label
<i>Ghisalberti and Nepf</i> [2004]	cylinders in water	solid diamond
<i>Dunn et al.</i> [1996], runs 1, 2, 4, 8, 10, 13, 15, 18	cylinders in water	solid square
<i>Nepf and Vivoni</i> [2000], runs 6 and 7	cylinders in water	solid circle
<i>Tsujimoto et al.</i> [1992], R43, A11, A31, A71	cylinders in water	solid triangle
<i>Murphy</i> [2006]	cylinder in water	open circle
<i>Seginer et al.</i> [1976], unconfined case	cylinders in air	cross with label
<i>Raupach et al.</i> [1986]	rectangular strips in air	open triangle
<i>Brunet et al.</i> [1994]	flexible, cylinders in air	open diamond
<i>Katul and Chang</i> [1999]	pine forest, $C_D = 0.2$	star with label
<i>Shaw et al.</i> [1974]	corn, $C_D = 0.35$	star with label
<i>Wilson</i> [1988]	corn, $C_D = 0.3$	star with label
<i>Amiro</i> [1990]	pine and aspen, $C_D = 0.3$; spruce, $C_D = 0.15$; Figure 1	star with label

^aFor consistency with drag law given in (2), drag coefficients are adjusted for studies that exclude the factor 1/2.

Finally, the viscous dissipation, e_{ν} , is generally negligible relative to the canopy dissipation [*Wilson*, 1988].

[9] From the above discussion, only shear production and canopy dissipation contribute significantly to the kinetic energy budget at the shear layer scale. This suggests that the growth of the shear-layer-scale turbulence will be arrested, when shear production balances canopy dissipation, which implies,

$$\frac{\langle \bar{u} \rangle C_D a}{\partial \langle \bar{u} \rangle / \partial z} = - \frac{2 \langle \overline{u'w'} \rangle}{2 \langle \overline{u'^2} \rangle + \langle \overline{v'^2} \rangle + \langle \overline{w'^2} \rangle}. \quad (3)$$

The ratio of turbulent statistics on the right-hand side of (3) can be estimated from observations reported for several real and model canopies [*Dunn et al.*, 1996; *Nepf and Vivoni*, 2000; *Seginer et al.*, 1976; *Wilson*, 1988; *Katul and Chang*, 1999]. We assume that all measures of turbulence are dominated by the shear-scale turbulence, which is reasonable if $d \ll h$ [*Shaw and Seginer*, 1985]. From the literature the turbulence ratio is 0.20 ± 0.03 (standard deviation), which matches the value observed in free shear layers (0.21 [e.g., *Wyngnanski and Fielder*, 1970]), bearing out the similarity between free and canopy shear layers.

[10] We define the left-hand side of (3) as the canopy shear layer (CSL) parameter.

$$CSL = \frac{\langle \bar{u} \rangle C_D a}{\partial \langle \bar{u} \rangle / \partial z}. \quad (4)$$

In principle we wish to evaluate this parameter at the inflection point, where, by definition, the shear in the denominator is maximum. In practice, the inflection point is close to or indistinguishable from the top of the canopy. Experimental data was drawn from studies that provide profiles of both $\langle \bar{u} \rangle(z)$ and $\langle \overline{u'w'} \rangle(z)$ (Table 1). In each case C_D is reported or estimated from a momentum balance within the canopy (e.g., as by *Ghisalberti and Nepf* [2004]). We only consider cases for which $H/h > 2$, so that the flow depth does not restrict shear layer growth [*Nepf and Vivoni*, 2000]. Furthermore, we only consider cases for which $C_D a h > 0.1$, because sparser canopies do not generate an

inflection point, and thus do not produce the coherent shear layer vortices. The limit 0.1 is based on a series of canopies examined by *Dunn et al.* [1996] and *Poggi et al.* [2004a]. The Dunn profiles span $C_D a h = 0.02$ to 0.35, and the Poggi profiles [*Poggi et al.*, 2004a] span $C_D a h = 0.02$ to 0.6. Cases with $C_D a h < 0.04$ exhibited a boundary layer form with no inflection point. A pronounced inflection point appeared at the top of the canopy for $C_D a h > 0.1$. The limit $C_D a h > 0.1$ also satisfies the condition for negligible dispersive flux ($ah > 0.1$, discussed above) as $C_D \approx 1$ is fairly common.

[11] The values of CSL estimated from the data sources listed in Table 1 are plotted in Figure 2. CSL is statistically constant across several decades of canopy Reynolds' number, $Re_h = U_h h / \nu$, where U_h is the velocity at the top of the canopy. The value, $CSL = 0.23 \pm 0.06$ (standard deviation), is also consistent with the turbulence ratio given on the right-hand side of (3). Physically speaking, this agreement suggests that canopy shear layer vortices are constrained by a balance of shear production and dissipation by canopy drag. The parameter CSL represents a universal mean flow structure for canopy shear layers that, like free shear layers, are defined by the large coherent structures they produce. The equilibrium described by CSL is achieved at a short distance, $10h$, from the leading edge of a canopy (based on profiles measured by *Ghisalberti* [2000]).

[12] The parameter CSL provides an estimate for the length scale, δ_e . First, the velocity shear in the upper canopy can be approximated by the ratio U_h / δ_e , as shown in Figure 1. This approximation is best for dense canopies for which $U_1 \ll U_h$. Next, because the inflection point is close to $z = h$, $\langle \bar{u} \rangle \approx U_h$. Then (4) yields

$$\frac{\delta_e}{h} \approx \frac{CSL}{C_D a h}. \quad (5)$$

[13] This scale relation is supported by experimental data. Profiles of Reynolds' stress are used to define the penetration length scale δ_e . Reynolds' stress peaks near the top of the canopy (e.g., as in Figure 1) and decays downward into the canopy. The maximum extent of vortex penetration corresponds to the point at which turbulent stress becomes

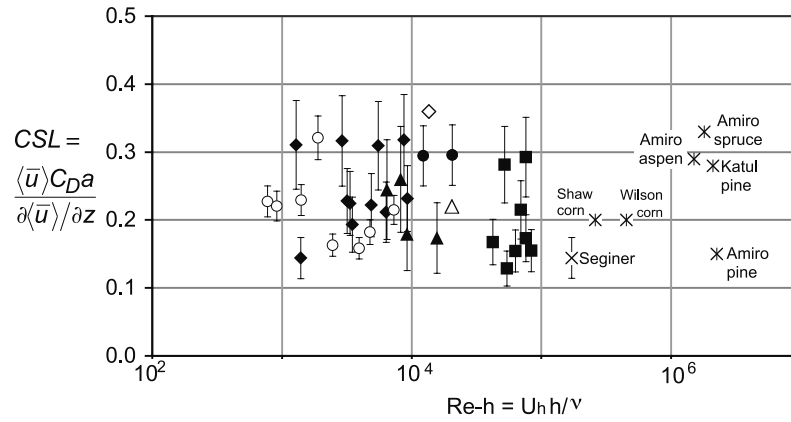


Figure 2. CSL equilibrium parameter defined in equation (4) estimated from data sources listed in Table 1. Because U_h is not provided for Katul pine, for plotting purposes we take $U_h = 1.5$ m/s, as in Amiro pine.

negligible. In practice, we chose the vertical position at which Reynolds' stress decays to 10% of its peak value, and δ_e is taken as the distance from the top of the canopy to this point. The measured penetration scale normalized by the canopy height (δ_e/h) is shown in Figure 3, plotted versus the momentum absorption scale, also normalized by the canopy height, $(C_D a h)^{-1}$. The dashed lines represent equation (5) for $CSL = 0.17$ and 0.29 , i.e., one standard deviation below and above the mean value (0.23), respectively. These lines bound nearly all observations of penetration scale, supporting the relation given by equation (5). This result indicates that the penetration scale (δ_e) is determined by canopy morphology, expressed through the momentum absorption scale ($C_D a$), and it is independent of flow speed, except through the Re_d dependence of C_D and a (e.g., through changes in pronation). This result is similar to one obtained by *Beavers and Joseph* [1967], who found that the penetration length of streamwise velocity into a porous channel bed was proportional to $\sqrt{k_p}$, where k_p is the permeability of the medium. Here $(C_D a)^{-1}$ plays the role of the permeability. Finally, Figure 3 suggests that for $(C_D a h)^{-1} > \approx 5$ (or $C_D a h \approx < 0.2$), the vortex penetrates to the bed, i.e., $\delta_e = h$. Canopies up to $(C_D a h)^{-1} = 70$ consistently indicate $\delta_e/h = 1$. They are excluded from the graph to emphasize the lower values of $(C_D a h)^{-1}$. Given the power to predict δ_e , we can now develop a transport model based on this scale.

3. Two-Box Model for Canopy Flushing

[14] The length scale δ_e divides the canopy into two regions, suggesting a two-box model (Figure 4). The upper canopy, $h - \delta_e < z < h$, is called the exchange zone, because it exchanges rapidly with the overflow through the direct action of the shear-scale vortices (gray region in Figure 4). The powerful, shear-scale turbulence does not penetrate the lower canopy, so that transport in the region $z < h - \delta_e$ (called the wake zone) is limited to small-scale turbulence generated in stem wakes (black region in Figure 4). The equations to predict transport in each region are developed below.

[15] The shear layer vortices control the turbulent exchange of mass across the canopy interface ($z = h$), and may be characterized by an exchange velocity k_e . In a set of

experiments spanning $C_D a h = 0.26$ to 0.65 , *Ghisalberti and Nepf* [2005] have shown that k_e is proportional to ΔU , the vortex velocity scale,

$$k_e = \Delta U / 40. \tag{6}$$

Because the shear-scale vortices also control the turbulent exchange of momentum, one can infer from mixing length theory that the turbulent stress at the top of the canopy $-\langle u'w' \rangle_{z=h}$, will scale with $(\Delta U)^2$. We define the friction velocity at the top of the canopy as $u_{*h} = (\langle u'w' \rangle_{z=h})^{1/2}$. The ratio $\Delta U / u_{*h}$ was evaluated with data sets from *Ghisalberti and Nepf* [2004], *Murphy* [2006], *Nepf and Vivoni* [2000], and *Dunn et al.* [1996], as listed in Table 1 (Figure 5). The ratio $\Delta U / u_{*h}$ has some dependence on $C_D a h$ ($r = 0.78$, $N = 37$, $p < 0.05$ [*Taylor*, 1982, p. 248]). This is consistent with the decline in vortex penetration (δ_e) with increasing $C_D a h$. As the vortex scale decreases, the exchange of momentum is less efficient, the stress $\langle u'w' \rangle_{z=h}$ achieved for a given ΔU is then diminished, and the ratio $\Delta U / u_{*h}$

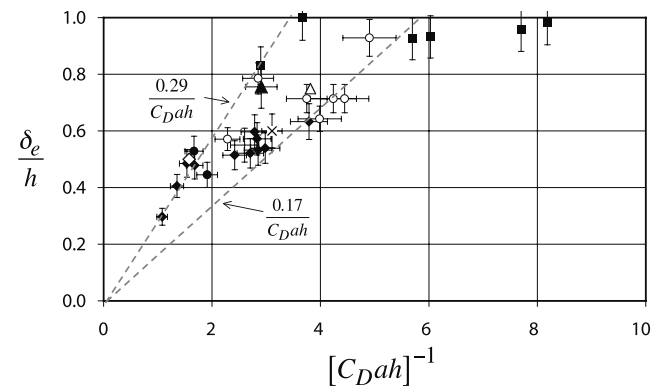


Figure 3. Normalized penetration scale, δ_e/h , versus scale parameter $(C_D a h)^{-1}$. Symbols indicate data source given in Table 1. The dashed lines show the linear relation given by equation (5) for $CSL = 0.17$ and 0.29 , i.e., one standard deviation below and above the mean observed value of $CSL = 0.23 \pm 0.06$, respectively.

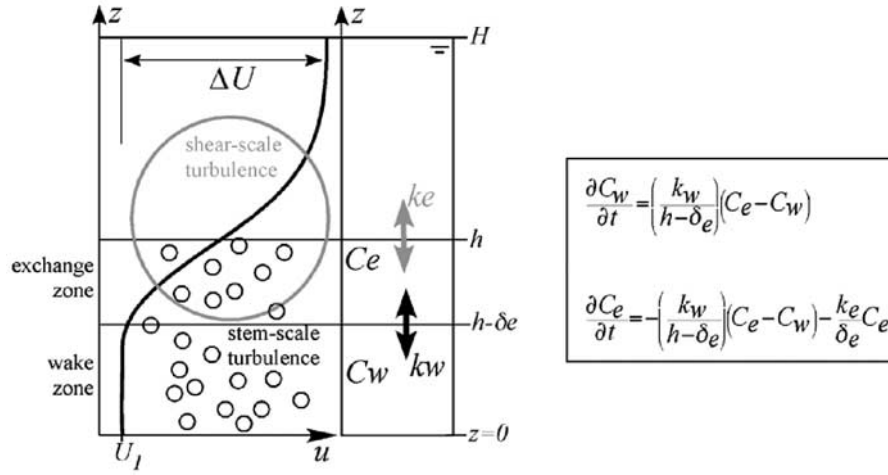


Figure 4. Plot showing how the length scale δ_e divides the canopy into two regions. In the exchange zone ($h - \delta_e < z < h$), shear scale turbulence (gray region) facilitates rapid exchange with the overflow, described by exchange velocity k_e (equation (8)). The shear-scale turbulence does not penetrate into the wake zone ($z < h - \delta_e$), so vertical transport in this region is limited to stem-scale turbulence (black region), which sets the wake zone exchange velocity, k_w (equations (10), (11), and (12)). The concentration in each zone evolves following the equations given at the right.

increases. For $H/h \geq 1.25$, the ratio $\Delta U/u_{*h}$ has no significant dependence on H/h (data not shown). Data for $H/h < 1.25$ was not available.

[16] A momentum balance for the water column above the canopy yields

$$(u_{*h})^2 = -\langle u'w' \rangle_{z=h} = -gS(H-h), \quad (7)$$

where the potential gradient, S , includes gradients in bed elevation (z_b) and hydrostatic pressure, i.e., $S = \partial z_b / \partial x + \partial H / \partial x$. Experimental observations confirm (7) within uncertainty, specifically $u_{*h} / \sqrt{-gS(H-h)} = 0.9 \pm 0.1$ (data not shown). Combining (6) and (7) with the empirical relation found in Figure 5, we can predict the exchange velocity from the boundary conditions, S , H , h , $C_D ah$.

$$k_e = 0.19u_{*h}(C_D ah)^{0.13} \quad (8)$$

This exchange velocity dictates the timescale of water renewal in the exchange zone, i.e., the exchange zone retention time.

$$T_{\text{exchange}} = \frac{\delta_e}{k_e} \quad (9)$$

[17] The exchange coefficient, k_e , and associated residence time, T_{exchange} , was developed from laboratory studies. A recent study in the Florida Everglades demonstrates its application in the field. *Harvey et al.* [2005] measured transport in a natural canopy of emergent (*Eleocharis cellulosa* and *Eleocharis elongata*) and submerged (*Utricularia purpurea* and *Utricularia foliata*) macrophytes. The submerged macrophytes floated beneath the water surface, forming a vegetative layer that was 20 cm thick. Beneath this floating mat the canopy consisted of a sparse distribu-

tion of *Eleocharis* stems, so that the flow was segregated into two zones, fast moving fluid in the stems and slow moving fluid in the floating mat. The velocity difference between these regions was $\Delta U = 0.5$ cm/s. Using equation (6) to predict k_e and assuming $\delta_e = 20$ cm, our model predicts a residence time in the floating mat of 30 min (equation (9)). From a tracer study the residence time within the floating mat was estimated to be 53 min. This reasonable agreement demonstrates how direct field measures of velocity can be used to estimate k_e .

[18] Next, consider the wake zone, $z < h - \delta_e$, which contains only stem-scale turbulence (black region in Figure 4). Field and laboratory studies have shown that the resulting turbulent diffusion scales on the stem diameter, d , and local

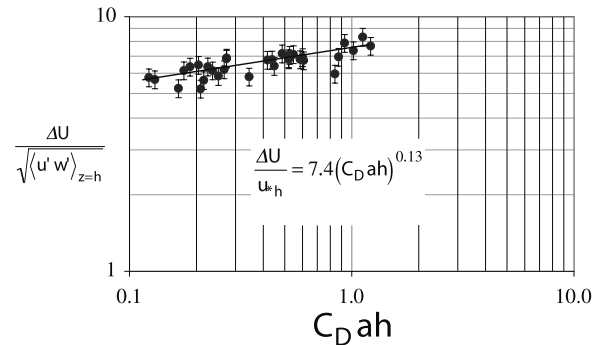


Figure 5. Ratio of vortex velocity scale (ΔU) and Reynolds stress $u_{*h} = \sqrt{\langle u'w' \rangle_{z=h}}$ versus the canopy drag parameter. Data are taken from *Ghisalberti and Nepf* [2004], *Murphy* [2006], *Nepf and Vivoni* [2000], and *Dunn et al.* [1996], as given in Table 1. A highly significant dependence on $C_D ah$ is shown ($r = 0.78$, 37 points, $p < 0.05$ [Taylor, 1982, p. 248]).

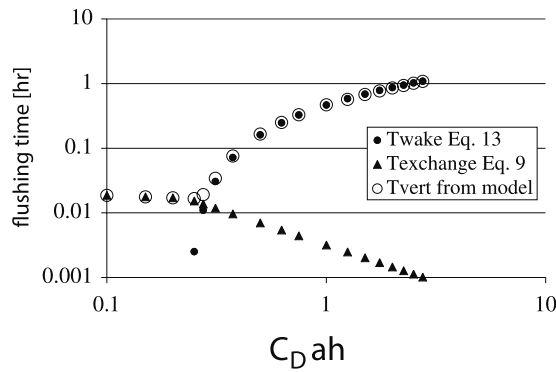


Figure 6. Flushing timescale calculated for $h = 25$ cm, $H/h = 4$, and $S = 10^{-4}$. For $C_D ah < 0.3$, vertical flushing is controlled by the exchange zone, and the model timescale matches that predicted from exchange zone parameters (equation (9)). For $C_D ah > 0.3$, vertical flushing is controlled by the wake zone, and the model timescale matches that predicted from wake zone parameters (equation (13)).

velocity $\langle \bar{u} \rangle$ [e.g., *Nepf, 1999; Lightbody and Nepf, 2006*]. Here we adopt the scale constant observed in field canopies [*Lightbody and Nepf, 2006*].

$$D_w = 0.17 \langle \bar{u} \rangle d = 0.17 U_1 d \quad (10)$$

In the two-box model, $\langle \bar{u} \rangle = U_1$, the velocity in the wake zone (Figure 4). As in an emergent canopy, the linear momentum in the wake zone reduces to a balance between potential gradient and canopy drag [*Lightbody and Nepf, 2006*], yielding

$$U_1 = \sqrt{\frac{2gS}{C_D a}} \quad (11)$$

With D_w given by equation (10), the exchange velocity at $z = h - \delta_e$ is

$$k_w = \frac{D_w}{h - \delta_e} \quad (12)$$

The water renewal time in the wake zone (wake zone retention time) is then

$$T_{wake} = \frac{(h - \delta_e)}{k_w} = \frac{(h - \delta_e)^2}{D_w} \quad (13)$$

The rightmost expression clarifies that the wake residence time is equivalent to the diffusion time for this region, since water renewal occurs through diffusion.

[19] The two-box model can now be used to evaluate the flushing (retention) time for a submerged canopy. Beginning with a uniform concentration in the canopy, $C_e = C_w = C_o$, a numerical scheme tracks the evolution of concentration in the exchange zone (C_e) and wake zone (C_w), using the following equations.

$$\begin{aligned} \frac{\partial C_w}{\partial t} &= \left(\frac{k_w}{h - \delta_e} \right) (C_e - C_w) \\ \frac{\partial C_e}{\partial t} &= - \left(\frac{k_w}{h - \delta_e} \right) (C_e - C_w) - \frac{k_e}{\delta_e} C_e \end{aligned} \quad (14)$$

This model assumes a uniform concentration within each box. This is reasonable in the exchange zone, because flushing here is driven by turbulence of a scale comparable to zone depth δ_e . In contrast, turbulence in the wake zone is smaller than the zone depth ($h - \delta_e$), so we expect gradients to develop. Specifically, the concentration in the upper part of the wake zone will decline more rapidly than the concentration at the bed. A mathematical model based on an *erfc* series can resolve the gradients within the wake zone. This model predicts a flushing time for the wake zone that is $1.3 T_{wake}$. Thus the simpler, uniform model (equation (14)) slightly underpredicts (by 30%) the residence time of the wake zone.

[20] The second line in equation (14) assumes a perfect sink above the canopy, $C(z > h) = 0$. This is reasonable because the velocity, and thus the removal by advection, is fast above the canopy. The temporal evolution of the mean canopy concentration, $C_m = (h - \delta_e)C_w + \delta_e C_e$, is fitted to an exponential decay to determine the overall flushing timescale by vertical transport, T_{vert} . This also represents the canopy retention time, if vertical transport is the dominant mechanism for water renewal.

[21] The model is run for a range of cases chosen to match field conditions. Canopy height in rivers is typically 5 to 100 cm [*Wu et al., 1999; Kouwen, 1990*]. The depth ratio H/h may span 1 to 10, and values of $C_D ah$ may span 0.01 to 10 [e.g., *Wu et al., 1999; Kouwen and Unny, 1973*]. We only consider $C_D ah \geq 0.1$, which is required to produce shear layer vortices, as described above. Finally, slope and surface gradients are typically in the range $S = 10^{-3}$ to 10^{-5} [e.g., *Dade and Friend, 1998*].

[22] Water within a canopy may also be renewed by longitudinal advection. For a canopy of length L , this process occurs in the timescale

$$T_{adv} = \frac{L}{U_c}, \quad (15)$$

where U_c is the vertically averaged velocity within the canopy. To understand whether vertical exchange or longitudinal advection control the overall canopy flushing time, T , we define the following transition length scale

$$L_T = U_c T_{vert}. \quad (16)$$

If canopy length $L < L_T$, then $T_{adv} < T_{verts}$, and water renewal (retention) is controlled by longitudinal advection, $T = T_{adv}$. If $L > L_T$ water renewal is controlled by vertical exchange $T = T_{vert}$.

4. Time and Length Scales of Canopy Water Renewal

[23] First consider the conditions $h = 25$ cm, $H/h = 4$, and $S = 10^{-4}$ (Figure 6). The vertical flushing time, T_{vert} , predicted from the model is shown as open circles. It ranges from a minute to an hour. As the canopy drag $C_D ah$ increases, T_{vert} initially decreases slowly, and then increases. The nonlinear behavior arises from a transition between exchange zone and wake zone dominance. For $C_D ah < 0.3$, T_{vert} is controlled by the exchange zone, and the model timescale matches that predicted from exchange zone

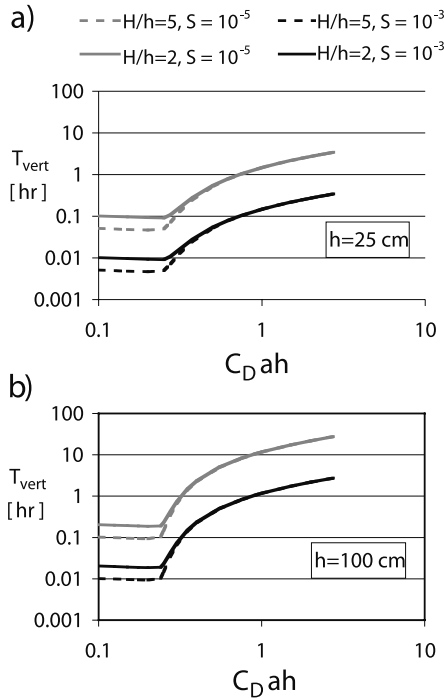


Figure 7. Vertical flushing time for (a) $h = 25$ cm and (b) $h = 100$ cm.

parameters, $T_{vert} = T_{exchange}$ given by equation (9). In this range the exchange zone fills all or nearly all of the canopy, with $\delta_e/h \approx 0.75$ at the transition $C_{Dah} = 0.3$ (from equation (5)). Because the flushing is set by $k_e \sim (C_{Dah})^{0.13}$ (equation (8)), T_{vert} decreases with increasing C_{Dah} in this range. For $C_{Dah} > 0.3$, the wake region is sufficiently large for the slow transport in this region to control vertical flushing, and $T_{vert} = T_{wake}$.

[24] Now consider flushing timescales over a range of field conditions: $h = 25$ and 100 cm, $H/h = 2$ and 5 , $S = 10^{-3}$ and 10^{-5} (Figure 7). A transition from exchange zone to wake zone dominance occurs close to $C_{Dah} = 0.3$ for all cases. The depth of submergence, H/h , is only important in the exchange zone regime ($C_{Dah} < 0.3$), as it affects k_e through u_{*h} (equation (8)). The majority of conditions produce canopy retention times of minutes to an hour, with the shortest, ≈ 1 min, occurring for the short canopy, $h = 25$ cm, under the strongest forcing, $S = 10^{-3}$ (Figure 7a). The longest timescale, $O(10)$ hours, occurs for the tall canopy, $h = 100$ cm, under the weakest forcing, $S = 10^{-5}$ (Figure 7b). For the later, it is likely that flushing by longitudinal advection will reduce the overall retention time (see discussion below).

[25] The timescales predicted by the model are consistent with canopy residence times inferred from tracer studies in a vegetated channel, 2.5 and 30 min [Sukhodolova et al., 2006]. They are also comparable to the retention time for sand bed forms, (10 cm, 10^2 s), and gravel bars, (100 cm, 10^3 s), but less than the retention time associated with bank or point bar exchange, (1–10 m, 10^5 s) from Figure 9 of Harvey and Wagner [2000]. This suggests that macrophytes contribute to hydrologic storage at the same level as small hyporheic features (10–100 cm). Further, Harvey et al. [2003] used tracer tests to measure channel storage in a naturally evolving stream over a 5-year period. They

observed an order of magnitude increase in storage area and an increase in storage zone residence time from 5 to 24 min. The increase in retention was attributed, in part, to an increase in aquatic vegetation. The estimates presented in Figure 7 could explain the additional 20 min of retention time observed in that study. Finally, Harvey et al. [2003] note that the increase in hydrologic retention is correlated with an increase in Darcy-Weisbach friction factor, f . A comparison of drag laws shows that $f \sim C_{Dah}$. Thus, similar to Harvey et al. [2003], the model results shown in Figure 7 suggest that over the full range of canopy drag, the retention time increases with increasing drag, C_{Dah} . More detailed observations are needed to show whether the nonlinear behavior near $C_{Dah} = 0.3$ is manifest in the field.

[26] The timescales shown in Figure 7 were used to estimate the canopy length at which the mechanism of flushing transitions from advection to vertical exchange, called the transition length scale L_T (Figure 8). First, as observed for T_{vert} (Figure 7), there is a minimum at $C_{Dah} \approx 0.3$, at which point there is a shift between exchange ($C_{Dah} < 0.3$) and wake ($C_{Dah} > 0.3$) zone control. The depth of submergence ($H/h = 2$ or 5 in Figure 8) has a small influence on L_T through u_{*h} . The greatest influence on L_T is from the canopy height, because T_{vert} increases with h for all conditions (Figure 7). Finally, the potential gradient, S , has negligible impact on L_T , because the canopy velocity $U_c \sim S^{1/2}$, but $T_{vert} \sim S^{-1/2}$, so that the effects cancel in $L_T = U_c T_{vert}$. The curves for $S = 10^{-3}$ and 10^{-5} overlap. The conditions summarized in Figure 8 suggest a minimum value around $L_T/h \approx 20$. That is, a canopy whose length is less than 20 times its height, $L < 20h$, will be flushed by longitudinal advection. Recalling that the development of full-scale vortices requires $L/h \approx 10$, this regime more likely extends to $L \leq 30h$. For $C_{Dah} < 0.3$, the flushing of canopies of length $L > 40h$ will be controlled by vertical exchange. Real canopies may range from $L/h = 4$ to over 100 [e.g., Fonseca et al., 1983; Sukhodolov and Sukhodolova, 2006], so that canopies flushed either by longitudinal advection or vertical exchange may occur in the field.

[27] The model described here could provide a tool for evaluating the fluid residence time within canopies of different morphology. The model components for wake zone diffusion [Lightbody and Nepf, 2006] and vortex-driven exchange [Harvey et al., 2005] (see also discussion

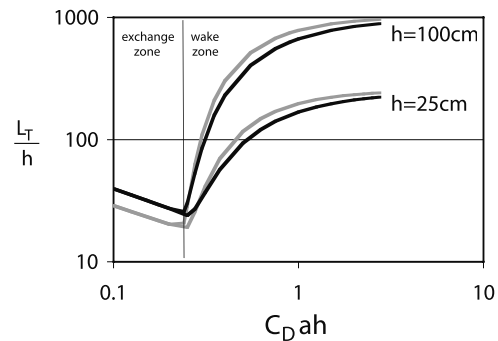


Figure 8. Transition canopy length, L_T , for canopy height $h = 25$ cm and 100 cm. Depth of submergence is $H/h = 2$ (black lines) and $H/h = 5$ (gray lines). The potential slope (S) has no influence on L_T , so that curves $S = 10^{-3}$ and 10^{-5} overlap.

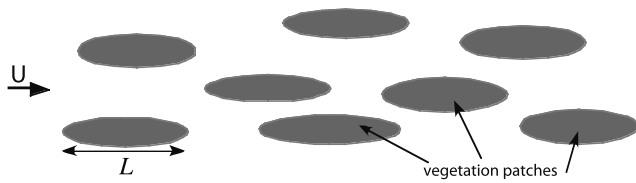


Figure 9. Top view of a river channel with patches of submerged vegetation. The patches have a characteristic length scale, L , and height, h . Water parcels that enter a patch are delayed relative to the free stream. The accumulation of transient storage events within multiple patches produces to longitudinal dispersion.

above) are supported by field observations. However, further studies are needed to test and refine the full model for field application. Tracer studies, such as described by *Harvey et al.* [2005] and *Sukhodolova et al.* [2006], can provide direct estimates of canopy residence time. This type of study should be extended to include measures of momentum absorption scale C_{Dah} . If velocity profiles can be made within the canopy, a direct measure of U_1 can be made [see, e.g., *Sukhodolova et al.*, 2006]. Then, using the observed U_1 , equation (11) provides a simple indirect measure of C_{Da} .

5. Implications for Longitudinal Dispersion

[28] Submerged vegetation creates regions of diminished flow that contribute to longitudinal dispersion via transient storage, also known as slow zone or dead zone dispersion [e.g., *Day*, 1975; *Valentine and Wood*, 1977; *Smith*, 1981; *Chikwendu and Ojiakor*, 1985]. Consider a channel with patches of submerged vegetation. Each patch has a characteristic length, L , and height, h (Figure 9). Water parcels that enter a patch will be delayed and subsequently separated longitudinally from parcels that remain in the open water. After a sufficient time and length scales that allows all water parcels to sample some patches, this process converges to a Fickian limit with constant dispersion coefficient K_x . This limit is generally reached over length scales much greater than the patch lengths, i.e., $> O(10 L)$. Even though the Fickian limit is not always reached in the field, it is a useful benchmark for understanding scale dependencies even in pre-Fickian conditions. The dispersion resulting from patches of vegetation is proportional to the velocity difference between the vegetation and the open water (ΔU), and the timescale required to sample a patch, T . In the Fickian limit, the constant dispersion coefficient is

$$K_x \sim (\Delta U)^2 T. \quad (17)$$

In the preceding section, we established that T is set either by longitudinal advection ($T = T_{adv}$), or by vertical exchange ($T = T_{vert}$). Furthermore, for the latter, either the exchange zone ($T_{vert} = T_{exchange}$) or the wake zone ($T_{vert} = T_{wake}$) determines canopy retention time. Let us consider the scale of K_x in each of these regimes. First, consider flushing by advection, such that $T = T_{adv} = L/U_c$ in equation (17). Then,

$$K_x = \frac{\Delta U}{U_c} \Delta U L \quad \text{for } T = T_{adv} \quad (18)$$

From equations (7) and (11) and Figure 5, the ratio $\Delta U/U_1 \sim (C_{Dah})^{0.63}$. Since $U_c \sim U_1$, we anticipate that $\Delta U/U_c$ is also function of C_{Dah} . However, the principal result is that for a given canopy type (C_{Dah} fixed), ΔU and U_c are fixed, so that the longitudinal dispersion depends on canopy patch length, i.e., $K_x \sim L$.

[29] Next, consider $T = T_{exchange}$, for which $C_{Dah} < 0.3$ and we approximate $\delta_e = h$, so that $T = T_{exchange} \approx h/k_e = 40h/\Delta U$ (equations (6) and (9)). Substituting into equation (17),

$$K_x = 40 \Delta U h \quad \text{for } T = T_{exchange} \quad (19)$$

Note the scale shift, from L to h dependence, as a canopy transitions from longitudinal (equation (18)) to vertical (equation (19)) flushing. The velocity jump $\Delta U \sim (C_{Dah})^{0.13}$ (Figure 5), and thus $\Delta U = f(h)$, such that the dependency between K_x and h may be nonlinear, i.e., more precise correlation may be found with $K_x \sim h^m$, with $m > 1$.

[30] Finally, consider $T = T_{wake}$. This requires $C_{Dah} > 0.3$, for which we approximate $\delta_e = 0$, and $T_{wake} \approx h^2/(U_1 d)$ from equations (10), (12), and (13). Substituting into (17)

$$K_x = \left[\frac{h \Delta U^2}{d U_1} \right] h \quad \text{for } T = T_{wake} \quad (20)$$

The ratio h/d is nearly a constant, based on geometric similarity observed among aquatic plants [*Niklas*, 1994]. From equation (11) and Figure 5, the ratio $\Delta U^2/U_1$ is a weak function of C_{Dah} , and thus h . Specifically, $(\Delta U)^2/U_1 \sim (C_{Dah})^{0.76}$. So, as with exchange zone scaling (equation (19)), we cannot conclude an exact form of the dependency between K_x and h in this regime. Nonetheless, in both regimes controlled by vertical flushing (equations (19) and (20)), the simple result is that $K_x \sim h$, in contrast to $K_x \sim L$ in canopies flushed by longitudinal advection. The transition between these dispersion regimes is depicted in Figure 10, with the boundaries of each regime set by the canopy length (L), height (h), and the momentum absorption (C_{Dah}).

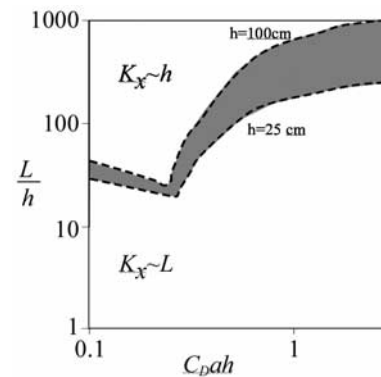


Figure 10. Regime of longitudinal dispersion, which depends on the patch length, L . In short canopies (L/h small) the canopy contribution to longitudinal dispersion scales with the canopy length. In long canopies (L/h large), longitudinal dispersion scales with the canopy height. The boundary between regimes depends on the canopy height, as indicated by the dashed lines marked $h = 25$ and 100 cm.

Figure 10 can guide future studies of dispersion in vegetated channels, by delineating under which conditions h versus L dependencies can be expected.

6. Conclusion

[31] Vertical transport in submerged canopies is prescribed by two distinct scales of turbulence: shear-scale turbulence generated at the top of the canopy and stem-scale turbulence generated within the canopy. When the canopy drag is small, $C_{Dah} < 0.3$, shear-scale turbulence penetrates far into the canopy, and water renewal occurs over time-scales of minutes to tens of minutes (Figure 7). When the canopy is dense ($C_{Dah} > 0.3$), the shear-scale turbulence cannot penetrate far into the canopy, and vertical flushing is controlled by the stem-scale turbulence, such that the flushing timescale is much longer, on the order of hours. In the later case, water renewal may occur first through longitudinal advection. The impact of canopy retention on longitudinal dispersion is determined by the mode of flushing, with dispersion scaling on the canopy height or length for vertical and longitudinal flushing, respectively.

[32] **Acknowledgments.** This material is based upon work supported by the National Science Foundation under grant EAR0309188. Any opinions, conclusions, or recommendations expressed in this material are those of the author(s) and do not necessarily reflect the views of the National Science Foundation.

References

- Amiro, B. D. (1990), Drag coefficients and turbulence spectra within three boreal forest canopies, *Boundary Layer Meteorol.*, *52*, 227–246.
- Beavers, G., and D. Joseph (1967), Boundary conditions at a naturally permeable wall, *J. Fluid Mech.*, *30*, 197–207.
- Brown, G. L., and A. Roshko (1974), On density effects and large structure in turbulent mixing layers, *J. Fluid Mech.*, *64*, 775–816.
- Brunet, Y., J. Finnigan, and M. Raupach (1994), A wind tunnel study of air-flow in waving wheat: Single-point velocity statistics, *Boundary Layer Meteorol.*, *70*, 95–132.
- Chambers, P., and E. Prepas (1994), Nutrient dynamics in riverbeds: The impact of sewage effluent and aquatic macrophytes, *Water Res.*, *28*, 453–464.
- Chikwendu, S., and G. Ojiakor (1985), Slow-zone model for longitudinal dispersion in two-dimensional shear flows, *J. Fluid Mech.*, *152*, 15–38.
- Dade, B., and P. Friend (1998), Grain-size, sediment transport regime, and channel slope in alluvial rivers, *J. Geol.*, *106*, 661–675.
- Day, T. (1975), Longitudinal dispersion in natural channels, *Water Resour. Res.*, *11*(6), 909–918.
- Dunn, C., F. Lopez, and M. Garcia (1996), Mean flow and turbulence in a laboratory channel with simulated vegetation, *Hydraulic Eng. Ser. 51*, U. of Ill. At Urban-Champaign, Urbana.
- Dwyer, M. J., E. G. Patton, and R. H. Shaw (1997), Turbulent kinetic energy budgets from a large-eddy simulation of airflow above and within a forest canopy, *Boundary Layer Meteorol.*, *84*, 23–43.
- Fonseca, M., J. Ziemann, G. Thayer, and J. Fischer (1983), The role of current velocity in structuring eelgrass meadows, *Coastal Shelf Sci.*, *17*, 367–380.
- Ghisalberti, M. (2000), Mixing layers and coherent structures in vegetated aquatic flows, M. S. thesis, Mass. Inst. of Technol., Cambridge.
- Ghisalberti, M., and H. Nepf (2002), Mixing layers and coherent structures in vegetated aquatic flow, *J. Geophys. Res.*, *107*(C2), 3011, doi:10.1029/2001JC000871.
- Ghisalberti, M., and H. Nepf (2004), The limited growth of vegetated shear-layers, *Water Resour. Res.*, *40*, W07502, doi:10.1029/2003WR002776.
- Ghisalberti, M., and H. Nepf (2005), Mass transfer in vegetated shear flows, *Environ. Fluid Mech.*, *5*(6), 527–551, doi:10.1007/s10652-005-0419-1.
- Harvey, J., and B. Wagner (2000), Quantifying hydrologic interactions between streams and their subsurface hyporheic zones, in *Streams and Groundwater*, edited by J. Jones, and P. Mulholland, pp. 3–44, Elsevier, New York.
- Harvey, J., M. Conklin, and R. Koelsch (2003), Predicting changes in hydrologic retention in an evolving semi-arid alluvial stream, *Adv. Water Resour.*, *26*, 939–950.
- Harvey, J., J. Saiers, and J. Newlin (2005), Solute transport and storage mechanisms in wetlands of the Everglades, south Florida, *Water Resour. Res.*, *41*, W05009, doi:10.1029/2004WR003507.
- Katul, G., and W.-H. Chang (1999), Principal length scales in second-order closure models for canopy turbulence, *J. Appl. Meteorol.*, *38*, 1631–1643.
- Katul, G., P. Wiberg, J. Albertson, and G. Hornberger (2002), A mixing layer theory for flow resistance in shallow streams, *Water Resour. Res.*, *38*(11), 1250, doi:10.1029/2001WR000817.
- Kouwen, N. (1990), Modern approach to design of grassed channels, *J. Irrig. Drain.*, *118*(5), 733–743.
- Kouwen, N., and T. Unny (1973), Flexible roughness in open channels, *J. Hydraul. Div. Am. Soc. Civ. Eng.*, *99*(HY5), 713–728.
- Lightbody, A., and H. Nepf (2006), Prediction of velocity profiles and longitudinal dispersion in emergent salt marsh vegetation, *Limnol. Oceanogr.*, *51*(1), 218–228.
- Mars, M., M. Kuruvilla, and H. Goen (1999), The role of submergent macrophyte *Triglochin huegelii* in domestic greywater treatment, *Ecol. Eng.*, *12*, 57–66.
- Murphy, E. (2006), Longitudinal dispersion in vegetated aquatic flow, M. S. thesis, Mass. Inst. of Technol., Cambridge, Mass.
- Nepf, H. (1999), Drag, turbulence, and diffusion in flow through emergent vegetation, *Water Resour. Res.*, *35*(2), 479–489.
- Nepf, H., and E. Vivoni (2000), Flow structure in depth-limited, vegetated flow, *J. Geophys. Res.*, *105*, 547–557.
- Niklas, K. (1994), The scaling of plant and animal body mass, length, and diameter, *Evolution*, *48*(1), 44–54.
- Poggi, D., A. Porporato, L. Ridolfi, J. Albertson, and G. Katul (2004a), The effect of vegetation density on canopy sub-layer turbulence, *Boundary Layer Meteorol.*, *111*, 565–587.
- Poggi, D., G. Katul, and J. Albertson (2004b), A note on the contribution of dispersive fluxes to momentum transfer within canopies, *Boundary Layer Meteorol.*, *111*, 615–621.
- Poggi, D., G. Katul, and J. Albertson (2004c), Momentum transfer and turbulent kinetic energy budgets within a dense model canopy, *Boundary Layer Meteorol.*, *111*, 589–614.
- Raupach, M., and R. Shaw (1982), Averaging procedures for flow within vegetation canopies, *Boundary Layer Meteorol.*, *22*, 79–90.
- Raupach, M., P. Coppin, and B. Legg (1986), Experiments on scalar dispersion in a model plant canopy: The turbulence structure, *Boundary Layer Meteorol.*, *35*, 21–52.
- Raupach, M., J. Finnigan, and Y. Brunet (1996), Coherent eddies and turbulence in vegetation canopies: The mixing-layer analogy, *Boundary Layer Meteorol.*, *60*, 375–395.
- Sand-Jensen, K. (1998), Influence of submerged macrophytes on sediment composition and near-bed flow in lowland streams, *Freshwater Biol.*, *39*, 663–679.
- Schultz, M., H.-P. Kozerski, T. Pluntke, and K. Rinke (2002), The influence of macrophytes on sedimentation and nutrient retention in the lower River Spree (Germany), *Water Res.*, *37*, 569–578.
- Seginer, I., P. Mulhearn, E. Bradley, and J. Finnigan (1976), Turbulent flow in a model plant canopy, *Boundary Layer Meteorol.*, *10*, 423–453.
- Shaw, R., and I. Seginer (1985), The dissipation of turbulence in plant canopies, paper presented at the 7th Symposium on Turbulence and Diffusion, Am. Meteorol. Soc., Boulder, Colo.
- Shaw, R., R. Silversides, and G. Thurtell (1974), Some observations of turbulence and turbulent transport within and above plant canopies, *Boundary Layer Meteorol.*, *5*, 429–449.
- Smith, R. (1981), A delay-diffusion description for contaminant dispersion, *J. Fluid Mech.*, *105*, 469–486.
- Sukhodolov, A., and T. Sukhodolova (2006), Evolution of the mixing layers in turbulent flow over submersed vegetation, paper presented at River Flow 2006, International Conference on Fluvial Hydraulics, Inst. Super. T c., Lisbon, 6–8 Sept.
- Sukhodolova, T., A. Sukhodolov, H.-P. Kozerski, and J. K hler (2006), Longitudinal dispersion in a lowland river with submersible vegetation, paper presented at River Flow 2006, International Conference on Fluvial Hydraulics, Inst. Super. T c., Lisbon, 6–8 Sept.
- Taylor, J. (1982), *An Introduction to Error Analysis*, Oxford Univ. Press, New York.
- Triska, F., R. Kennedy, G. Zellweger, and K. Bencala (1989), Retention and transport of nutrients in a third-order stream, *Ecology*, *70*, 1877–1892.
- Tsujimoto, T. (2000), Fluvial processes in streams with vegetation, *J. Hydraul. Res.*, *37*(6), 789–804.

- Tsujimoto, T., Y. Shimizu, T. Kitamura, and T. Okada (1992), Turbulent open-channel flow over bed covered by rigid vegetation, *J. Hydrosol. Hydraul. Eng.*, 10(2), 13–25.
- Valentine, E., and I. Wood (1977), Longitudinal dispersion with dead zones, *J. Hydraul. Div. Am. Soc. Civ. Eng.*, 103, 975–990.
- Wilcock, R., P. Champion, J. Nagels, and G. Crocker (1999), The influence of aquatic macrophytes on the hydraulic and physicochemical properties of a New Zealand lowland stream, *Hydrobiologia*, 416(1), 203–214.
- Wilson, N. (1988), A second-order closure model for flow through vegetation, *Boundary Layer Meteorol.*, 42, 371–392.
- Winant, C., and F. Browand (1974), Vortex pairing, the mechanism of turbulent mixing-layer growth, at moderate Reynolds number, *J. Fluid Mech.*, 63, 237–255.
- Wu, F.-C., H.-W. Shen, and Y.-J. Chou (1999), Variation of roughness coefficients for unsubmerged and submerged vegetation, *J. Hydraul. Eng.*, 125(9), 934–942.
-
- M. Ghisalberti, School of Environmental Systems Engineering, University of Western Australia, Crawley, WA 6009, Australia.
- E. Murphy and H. Nepf, Department of Civil and Environmental Engineering, Massachusetts Institute of Technology, 77 Massachusetts Avenue, Building 484, Room 2168, Cambridge, MA 02139, USA. (hmnepf@mit.edu)
- B. White, Woods Hole Oceanographic Institution, Woods Hole, MA 02543-1050, USA.